

# TFAP2A promotes cervical cancer via a positive feedback pathway with PD-L1

JUNYUAN YANG\*, YANG GAO\*, SINJIE YAO, SHIMENG WAN and HONGBING CAI

Department of Gynecological Oncology, Zhongnan Hospital of Wuhan University, Wuhan, Hubei 430071, P.R. China

Received December 2, 2022; Accepted April 10, 2023

DOI: 10.3892/or.2023.8551

**Abstract.** Transcription factor AP-2 alpha (TFAP2A) is a critical cell growth regulator that is overexpressed in various tumor tissues. However, its role in the development of cervical cancer remains unknown. In the present study, public databases were thus explored and a higher expression of TFAP2A was found in cervical cancer. A total of 131 clinical samples were collected and it was also identified that TFAP2A was highly expressed in cervical tumor tissues. TFAP2A was also found to be associated with a higher tumor stage, lymph node metastasis and a poor patient survival. *In vitro* experiments revealed that the knockdown of TFAP2A inhibited the proliferation and migration of cervical cancer cells and promoted apoptosis. Furthermore, it was observed that TFAP2A could bind the programmed death-ligand 1 (PD-L1) promoter region and PD-L1 rescued TFAP2A expression. *In vivo* experiments also revealed that TFAP2A promoted tumor growth. Collectively, in the present study it was demonstrated that TFAP2A is a transcription factor of PD-L1 and a prognostic factor with clinical value, identifying a positive feedback loop of TFAP2A/PD-L1.

## Introduction

Cervical cancer is a very lethal type of cancer with a high incidence and mortality (1), ~80% of them are cervical squamous cell carcinoma (2). Although in recent years, with the ongoing developments of treatment technologies and the broad availability of the HPV vaccine the incidence and mortality rate of cervical cancer have decreased (3), the therapeutic efficacy remains limited, and the main cause of the mortality of cervical cancer patients is the invasive metastasis of the tumor.

Therefore, the mining of molecular markers that can effectively modulate the invasive metastasis of cervical cancer may be beneficial in order to reduce the mortality rate of patients with cervical cancer.

TFAP2A is a crucial mediator of embryonic development that is aberrantly overexpressed in various types of cancer, including basal-squamous bladder cancer (4), pancreatic cancer (5), gastric cancer (6), lung adenocarcinoma (7), nasopharyngeal carcinoma (8) and ovarian cancer (9); TFAP2A mainly functions as a transcription factor that can promote the expression of particular genes, including direct upregulation of bone morphogenetic protein 4 (BMP4) promoting angiogenesis and leads to drug resistance (10) and induction of keratin 16 and transforming growth factor- $\beta$  (TGF- $\beta$ ) overexpression promoting the epithelial-mesenchymal transition of tumors (11,12). Accumulating evidence has demonstrated that TFAP2A has potential use as a diagnostic marker for specific tumors, and it is involved in cancer cell proliferation, invasion and migration (13). A high TFAP2A expression has been shown to be associated with a poor tumor prognosis and an increased risk of recurrence (14). It is also involved in tumor adaptability to hypoxia and food deprivation (8,15). The aforementioned findings suggested that TFAP2A is involved in cancer genesis and progression. However, the role of TFAP2A in cervical cancer remains unknown.

Programmed death-ligand 1 (PD-L1) is mainly expressed on the surface of tumor cells, and an increased PD-L1 expression is associated with the poor survival of cancer patients (16). In addition, its immunosuppressive signal activation results in the immunological tolerance in tumor cells (17) and it promotes tumor stem cell proliferation (18), indicating that PD-L1 is associated with cancer progression. Previously, immunosuppressants that target PD-L1 have exhibited exceptional efficacy in the treatment of cervical cancer (19). However, certain patients do not benefit from immunotherapy due to resistance. The response rate of PD-L1 antibodies for cervical cancer has been reported to be only ~20% (20). Therefore, there is a need for the understanding of the mechanisms regulating PD-L1 in tumors in order to address the limitations of current treatments. PD-L1 regulation is also diverse (21). At present, the association between TFAP2A and PD-L1 in cervical cancer is not clear and it would thus be of interest to investigate this.

In the present study, the expression of TFAP2A was first evaluated and it was found that it was highly expressed in

---

*Correspondence to:* Dr Hongbing Cai, Department of Gynecological Oncology, Zhongnan Hospital of Wuhan University, 169 Donghu Road, Wuchang, Wuhan, Hubei 430071, P.R. China  
E-mail: chb2105@163.com

\*Contributed equally

**Key words:** transcription factor AP-2 alpha, cervical cancer, programmed death-ligand 1, proliferation, migration

cervical cancer and was associated with a poor survival rate of patients with cervical cancer. Furthermore, it was identified that TFAP2A functions as the transcription factor of PD-L1 and PD-L1 can also elevate the expression of TFAP2A, which indicates a positive feedback loop between them. *In vivo* experiments demonstrated that the decreased expression of TFAP2A inhibited cervical tumor growth. The present study demonstrated that TFAP2A may function as a molecular marker for cervical cancer and revealed a positive feedback loop between TFAP2A and PD-L1.

## Materials and methods

**Data collection.** In the present study, four GSE datasets were used: GSE39001 (<https://www.ncbi.nlm.nih.gov/geo/query/acc.cgi?acc=GSE39001>), GSE63514 (<https://www.ncbi.nlm.nih.gov/geo/query/acc.cgi?acc=GSE63514>), GSE9750 (<https://www.ncbi.nlm.nih.gov/geo/query/acc.cgi?acc=GSE9750>) and GSE52903 (<https://www.ncbi.nlm.nih.gov/geo/query/acc.cgi?acc=GSE52903>). These datasets were utilized to evaluate the mRNA expression of TFAP2A between clinical cancer specimens and normal specimens. GSE52903 and The Cancer Genome Atlas (<https://xenabrowser.net/>) were used to analyze the association between TFAP2A and the clinicopathological characteristics of patients with cervical cancer, as well as to examine the link between TFAP2A and PDL1.

**Tissue sample collection.** Clinical samples, including 91 cervical cancer tissues and 30 normal cervical tissues, were obtained from the Zhongnan Hospital of Wuhan University (Wuhan, China) from January 2019 to December 2021. All procedures were approved (approval no. 2022120K) by the Ethical board of Zhongnan Hospital of Wuhan University (Wuhan, China). Of the 91 cervical cancer tissues, 80 were squamous carcinomas and 11 were adenocarcinomas.

**Cells and cell culture.** For the purposes of the present study, three human cervical cancer cell lines (HeLa, SiHa and C33a) and normal cervical epithelial cell lines (END1/E6E7) were selected. The cell lines were purchased from the American Type Culture Collection (ATCC). The cell culture medium consisted of 90% DMEM or RPMI-1640, 10% fresh inactivated fetal bovine serum (FBS; Gibco; Thermo Fisher Scientific, Inc.) and 1% penicillin-streptomycin solution (Thermo Fisher Scientific, Inc.). The culture conditions were set in an incubator with 5% CO<sub>2</sub>, 37°C and saturated humidity.

**Cell transfection.** PD-L1 and TFAP2A overexpression plasmids were constructed by inserting full-length cDNA (482 ng/ $\mu$ l) into target vectors (GV238 and GV710; Shanghai GeneChem Co., Ltd.). PD-L1 (591 ng/ $\mu$ l), TFAP2A (377 ng/ $\mu$ l), and HPV 16 E6 (483 ng/ $\mu$ l) short hairpin RNA were synthesized and cloned into pLKO.1 TRC (Shanghai GeneChem Co., Ltd.) vector to knock down the target genes. The aforementioned overexpression plasmids and gene knockdown plasmid were transfected into cervical cancer cells using Lipofectamine 2000® reagent (Invitrogen; Thermo Fisher Scientific, Inc.). The effects of plasmid transfection were detected after 48 h using western blot analysis. The sequences used are presented in Table SI.

**Reverse transcription-quantitative polymerase chain reaction (RT-qPCR).** TRIzol® reagent (Invitrogen; Thermo Fisher Scientific, Inc.) was used to collect and extract total RNA from the cervical cancer cells. Following 15 min (50°C, 10 min; 85°C, 5 min) of RNA reverse transcription (Prime Script™ RT Master Mix; used according to the manufacturer's protocol), the Ct values of the samples were monitored by qPCR. The thermocycling conditions were as follows: i) Pre-denaturation at 95°C for 30 sec; ii) cycle reaction (40 times) at 95°C for 10 sec and at 60°C for 30 sec; and dissolution curve: 95°C for 15 sec, 60°C for 60 sec, 15°C for 4 sec. SYBR-Green Master mix (Thermo Fisher Scientific, Inc.) was used for qPCR and data were calculated using the 2<sup>- $\Delta\Delta$ C<sub>q</sub></sup> method (22). GAPDH was used as the reference gene. The primers used are listed in Table SI.

**Western blot analysis.** After washing the cells with ice-cold PBS, protein lysate (RIPA lysate: PMSF ratio, 100:1; Beyotime Institute of Biotechnology) was added and collected. The BCA method (Tiangen Biotech Co., Ltd.) was used to measure the protein concentration. Protein loading buffer was added and boiled at 100°C and stored at -80°C. The exact amount of protein (30  $\mu$ g) was separated with 12% SDS-PAGE. The electrophoresis time was 1-1.5 h, and the proteins were then transferred onto PVDF membranes (Bio-Rad Laboratories, Inc.) and blocked with 5% skimmed milk at room temperature for 2 h. Corresponding diluted primary antibodies [PD-L1 (1:1,000), TFAP2A (1:1,000), GAPDH (1:5,000) and HPV 16 E6 (1:1,000)] were then added followed by overnight incubation at 4°C. An HRP-labeled secondary antibody (1:10,000) was then added and incubated at room temperature for 1 h. ECL chemiluminescence imaging system (Tanon-5200; Tanon Science and Technology Co., Ltd.) was used for imaging. The antibodies used for western blot analysis are listed in Table SII.

**Cell Counting Kit-8 (CCK-8) assay.** The transfected HeLa and SiHa cells were transferred into 96-well plates (5 $\times$ 10<sup>3</sup> cells/well) and 10  $\mu$ l/well of CCK-8 solution [Multisciences (Lianke) Biotech Co., Ltd] was added at 0, 24, 48, 72 and 96 h. The enzyme marker (PerkinElmer, Inc.) was used for detection of the absorbance at 450 nm after 2 h of incubation at 37°C.

**Wound healing assay.** The transfected HeLa and SiHa cells were laid flat in six-well plates (1 $\times$ 10<sup>5</sup> cells/well), and when the density reached ~60%, a wound was created in the cell monolayer using a 200- $\mu$ l pipette tip and marked and cultured with medium containing 2% FBS, followed by observation of the cells under a light microscope (Olympus Corporation) for 0 and 48 h and images were captured.

**Transwell assay.** Cellular migration and invasion were examined using Transwell assay. Cell invasion assays were performed in advance. The diluted Matrigel gel (BD Biosciences) was added to the Transwell chamber (Corning, Inc.) at 70  $\mu$ l/well and incubated at 37°C until set. Subsequently, 200  $\mu$ l cell dilution containing 1% FBS medium (1 $\times$ 10<sup>5</sup>/ml) were added to the upper chamber, while 800  $\mu$ l medium containing 10% FBS were added to the bottom chamber. Following 48 h of incubation at 37°C, the cells were subjected at room temperature to fixation 30 min with formaldehyde and crystal violet

(Beyotime Institute of Biotechnology) staining 20 min and placed under a fluorescent microscope (Olympus Corporation) to observe and obtain images for counting.

**Clonal formation assay.** The transfected cells were spread flat in six-well plates at a concentration of 300 cells/well, observed and cultured for 2 weeks. After the number of cells in the minimal clonal cell mass was >50, formaldehyde fixation for 30 min and 0.1% crystal violet solution staining for 20 min were performed and images were obtained by a fluorescent microscope (Olympus Corporation).

**Apoptosis detection.** The transfected cells were digested, resuspended and stained according to the instructions provided with the FITC Annexin V apoptosis detection kit [cat. no. AP104; Multisciences (Lianke) Biotech Co., Ltd.]. The number of apoptotic cells was immediately detected and counted using a flow cytometer (cut flex; Beckman Coulter, Inc.).

**Dual-luciferase reporter assays.** An overexpression plasmid (pGL3 plasmid) containing PD-L1 gene promoters of different lengths (P, P1, P2, P3, P4 and P5) and TFAP2A overexpression plasmid (pCDNA3.1 plasmid) were constructed. In 24-well plates, 0.5  $\mu$ g target plasmids and 0.01  $\mu$ g pRL-TK plasmid (Shanghai GeneChem Co., Ltd.) per well were co-transfected into 293T cells (ATCC) using Lipofectamine 2000<sup>®</sup> reagent (Invitrogen; Thermo Fisher Scientific, Inc.). The cells were analyzed to determine the activity of luciferase using a Dual-Luciferase<sup>®</sup> Reporter Assay System (Promega Corporation) following 48 h of transfection. Normalization was performed by comparison with *Renilla* luciferase activity.

**Chromatin immunoprecipitation (ChIP).** ChIP-qPCR primers containing the binding sequences of the PD-L1 promoter and TFAP2A gene were designed, and the cells were cross-linked with 1% formaldehyde, sonicated to fragment DNA, and the corresponding 4  $\mu$ g Ab or IgG and 50  $\mu$ l protein A/G-agarose (cat. no. 20421; MilliporeSigma) were then added for immunoprecipitation. The samples were washed and uncross-linked after rotating and mixing overnight at 4°C, and the PCR products were recovered using the PCR product recovery kit (the IP products were purified using the PCR product recovery kit; Tiangen Biotech Co., Ltd.), and finally RT-qPCR was performed using the designed primers, and positive controls were set to analyze the enriched DNA fragments (23). The primers used are listed in Table S1.

**Tumor xenograft model.** The animal experiment was approved (approval no. ZN2021257) by the Experimental Animal Ethics Committee of Zhongnan Hospital of Wuhan University (Wuhan, China). A total of 12 BALB/C nude mice (female, weighing 18-20 g, aged 4-6 weeks) were housed in an SPF-grade environment at the Animal Testing Center of the Central South Hospital of Wuhan University in Vital River, Beijing, China. The housing temperature was maintained at 22±2°C, with a relative humidity of 40-60%. A 12-h diurnal cycle was applied, and the mice were fed ad libitum with standard chow diet and water. All mice were experimented on after 1 week of acclimatization. The sh-TFAP2A and sh-NCs HeLa cells (5×10<sup>6</sup> cells, 100  $\mu$ l DMEM-containing

medium) were stably transfected with lentivirus and injected subcutaneously into the axilla of the nude mice. Tumor volume and mouse body weight were recorded every other day for ~18 days until tumor volume did not exceed 2,000 mm<sup>3</sup>. The mice were anesthetized with 1-1.5% isoflurane and euthanized by cervical dislocation. Tumors were excised from each mouse and their weights were calculated for statistical analysis. The tumor volume was calculated as follows: Volume=(length × width)<sup>2</sup>/2.

**Immunohistochemistry (IHC) and hematoxylin-eosin (H&E) staining.** The collected tumor tissues were fixed with 4% paraformaldehyde for 24 h at room temperature, alcohol-gradient dehydrated and paraffin-embedded and sectioned strictly according to the IHC staining and H&E staining procedures. The 4- $\mu$ m sections were then stained with antibodies against TFAP2A (1:450; cat. no. 67076-1-Ig; Proteintech Group, Inc.) and PD-L1 (1:150; cat. no. 66248-1-Ig; Proteintech Group, Inc.). Incubation was performed overnight at 4°C, and secondary antibodies [Goat Anti-Rabbit IgG H&L (HRP; 1:1,000; cat. no. ab6721; Abcam)] were used for re-staining at room temperature for 1 h followed by counterstaining (10-20 sec) with 1X hematoxylin solution (cat. no. DA1010; Beijing Solarbio Science & Technology Co., Ltd.) and mounting, followed by staining analysis, a procedure independently analyzed by two experienced pathologists. H&E staining solidifies the data to identify whether the tissue type is cervical cancer. The data of IHC staining were scored using a semi-quantitative scoring system. The average gray value of positive cells (staining intensity) and the percentage of positive areas (stained area) were used together as a measure of IHC staining, resulting in four scores: High positive (3+), positive (2+), low positive (1+) and negative (0). Finally, the scores of the three replicates were summed to obtain the final score; the median was used as a cut-off to distinguish between high and low protein expression.

**Statistical analysis.** SPSS 25.0 statistical software (IBM Corp.) was used for statistical analysis, GraphPad Version 5.0 Software (Dotmatics) for analysis and graphing, and ImageJ-win32 software (National Institutes of Health) for image analysis. Kaplan-Meier plotter followed by the log-rank test was used for survival analysis. Data are expressed as the mean ± SD, and the unpaired t-test was used for statistical analysis. P<0.05 was considered to indicate a statistically significant difference.

## Results

**TFAP2A is highly expressed in cervical cancer tissues and is associated with the clinicopathological features of patients.** The analysis results of multiple cervical cancer RNA-sequencing datasets in the Gene Expression Omnibus database suggested that the expression level of TFAP2A was significantly higher in cervical cancer tissues than in normal cervical tissues (Fig. 1A-D). In addition, seven sets of paired cancer-paraneoplastic tissues were collected and TFAP2A gene expression was evaluated. The results from RT-qPCR further supported the data mining results (Fig. 1E). Furthermore, 30 normal cervical tissues and 91 cervical cancer tissues were

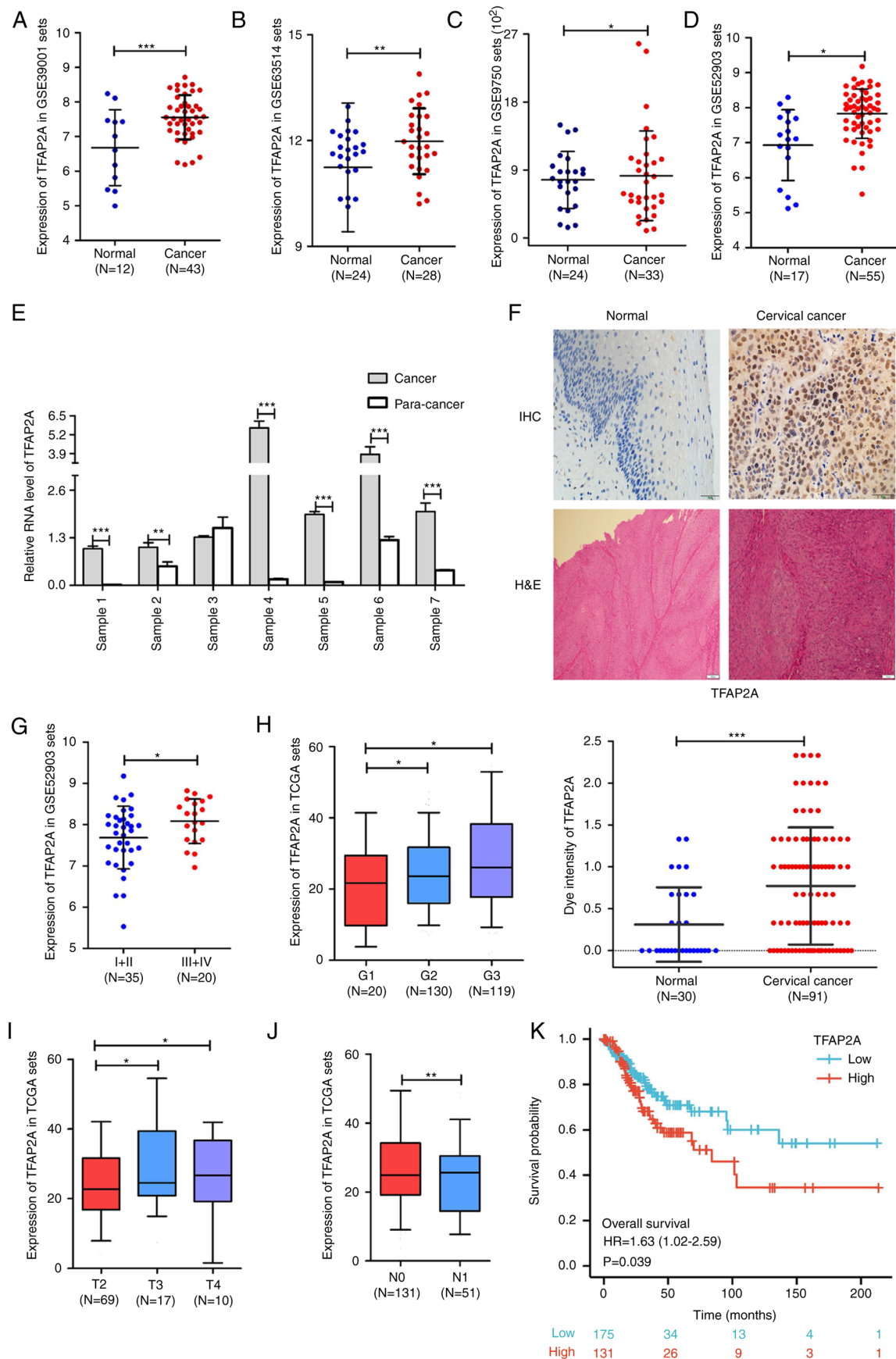


Figure 1. TFAP2A expression is increased in cervical cancer and is associated with clinicopathological features. (A-D) Analysis of TFAP2A mRNA expression in different datasets. (E) Expression of TFAP2A mRNA in six sets of paired cancer-paraneoplastic tissue samples. (F) IHC staining of TFAP2A expression and H&E staining in normal and cancer tissues. (G) Analysis of TFAP2A mRNA expression in different FIGO grades. (H) The expression level of the TFAP2A gene in different histopathology grades. (I) The expression level of TFAP2A gene in different FIGO T Stages. (J) The expression level of the TFAP2A gene according to lymph node metastasis. (K) The expression level of TFAP2A gene in association with patient survival. in each group. \*P<0.05, \*\*P<0.01 and \*\*\*P<0.001. TFAP2A, transcription factor AP-2 alpha; H&E, hematoxylin-eosin; IHC, immunohistochemical.



Table I. Association between TFAP2A and the clinicopathological parameters of patients with cervical cancer.

Clinicopathological characteristics	Expression level of TFAP2A		P-value
	Low	High	
Total cases, n (%)	46	45	
Age, years			0.159
≤55	24 (26.4%)	30 (33.0%)	
>55	22 (24.2%)	15 (16.5%)	
Underlying diseases			0.763
Yes	35 (38.5%)	33 (36.3%)	
No	11 (12.1%)	12 (13.2%)	
Pregnancy			0.599
≤3	22 (24.1%)	24 (26.4%)	
>3	24 (26.4%)	21 (23.1%)	
Childbirth			0.014
≤2	27 (30.0%)	37 (40.7%)	
>2	19 (20.9%)	8 (8.8%)	
CEA (ng/ml)			0.526
≤5	40 (45.0%)	39 (43.9%)	
>5	4 (4.5%)	6 (6.7%)	
CA125 (U/ml)			0.080
≤35	38 (43.2%)	44 (50.0%)	
>35	5 (5.7%)	1 (1.1%)	
HE4 (pmol/ml)			0.044
≤60.5	32 (41.6%)	25 (50.6%)	
>60.5	6 (7.8%)	14 (18.2%)	
SCC (ng/ml)			0.193
≤1.5	6 (8.0%)	12 (16.0%)	
>1.5	29 (38.7%)	28 (37.3%)	
FIGO stage			0.043
Ib-IIa	39 (43.3%)	31 (34.4%)	
IIB-IV	6 (6.7%)	14 (15.6%)	
HPV infection			0.013
Negative	12 (13.2%)	3 (3.3%)	
Positive	34 (37.4%)	42 (46.2%)	
Lymph node metastasis			0.534
Yes	5 (5.8%)	7 (8.1%)	
No	38 (44.2%)	36 (41.9%)	
Vascular invasion			0.006
Yes	18 (28.1%)	8 (12.5%)	
No	13 (20.3%)	25 (39.1%)	
Nerve Violation			0.772
Yes	18 (34.6%)	20 (38.5%)	
No	6 (11.5%)	8 (15.4%)	

TFAP2A, transcription factor AP-2 alpha; SCC, squamous cell carcinoma; CEA, carcinoembryonic antigen; HE4, human epididymis protein 4.

collected for IHC and H&E staining to further assess TFAP2A gene expression. The results suggested that the positive staining of TFAP2A was significantly higher in the cancerous tissues than in normal tissues (Fig. 1F). At the same time, the analysis

of the database cervical cancer samples revealed that patients with high levels of TFAP2A mRNA expression had a higher FIGO grade (Fig. 1G), a higher pathological stage (Fig. 1H) and a larger tumor size (Fig. 1I), as well as more lymph node

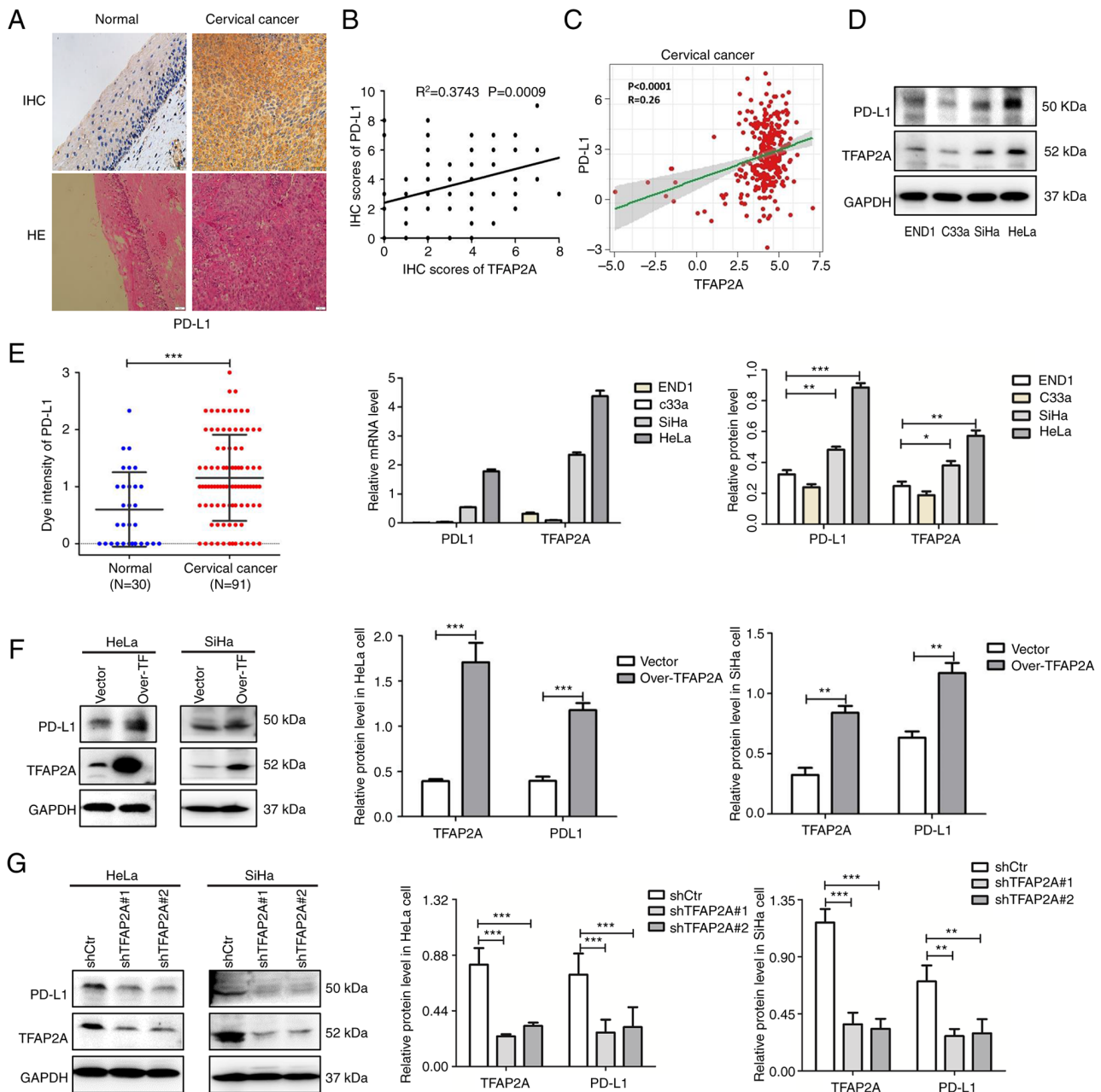


**Figure 2.** TFAP2A positively regulates PD-L1 expression in cervical cancer. (A) IHC staining of PD-L1 expression and hematoxylin-eosin staining in normal and cancer tissues. (B) The association between PD-L1 and TFAP2A protein (semi-quantitative analysis using IHC staining). (C) The association between PD-L1 and TFAP2A protein in The Cancer Genome Atlas database. (D) Western blot analysis of TFAP2A and PD-L1 expression in normal (END1) and cervical epithelial (HeLa, C33a and SiHa) cell lines. (E) Reverse transcription-quantitative PCR of TFAP2A and PD-L1 expression in normal (END1) and cancer) cervical epithelial (HeLa, C33a and SiHa) cell lines. (F) Western blot analysis revealed that PD-L1 expression was reduced in TFAP2A-overexpressing cervical cancer cell lines. (G) Western blot analysis revealed that PD-L1 expression was reduced in cervical cancer cell lines subjected to TFAP2A knock-down.  $n=3$  for cell culture analysis. \* $P<0.05$ , \*\* $P<0.01$  and \*\*\* $P<0.001$ . TFAP2A, transcription factor AP-2 alpha; PD-L1, programmed death-ligand 1; H&E, hematoxylin-eosin; IHC, immunohistochemical.

metastases when compared with those with a low TFAP2A expression (Fig. 1J). Kaplan-Meier survival analysis revealed that a high expression of TFAP2A was positively associated with a poor overall survival of patients with cervical cancer (Fig. 1K). It was also validated in clinical samples, as shown in Table I, that patients with a high TFAP2A expression exhibited fewer births, higher human epididymis protein 4 levels, a higher FIGO grade, more HPV infections, and were more prone to vascular invasion. These findings suggested that TFAP2A is highly expressed in cervical cancer tissues and is

associated with the clinical characteristics and prognosis of patients with cervical cancer.

*TFAP2A positively regulates PD-L1 expression in cervical cancer tissues and cell lines.* The IHC staining results of 30 normal cervical tissues and 91 cervical cancerous tissues revealed that positive PD-L1 staining was significantly higher in cancerous tissues than in normal tissues (Fig. 2A). Combined with the database analysis, a significant positive association was identified between PD-L1 and TFAP2A protein expression (Fig. 2B and C).

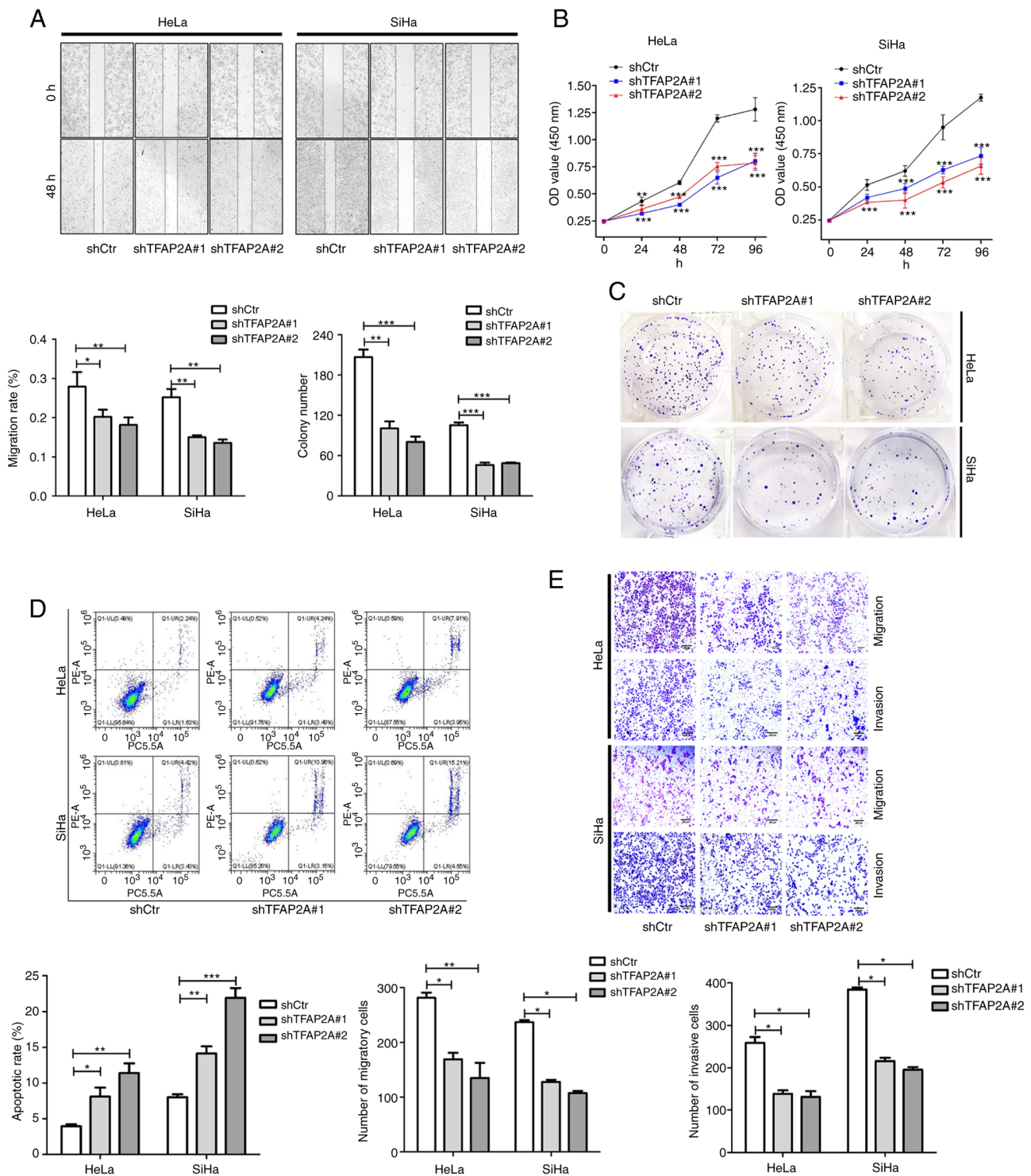


Figure 3. Knockdown of TFAP2A inhibits the proliferation, migration and invasion, and promotes the apoptosis of cervical cancer cells. (A) Wound healing assay revealed that the downregulation of TFAP2A significantly reduced the cell migration rate. Representative images were obtained at 48 h. Scale bars, 100  $\mu$ m. (B) Cell Counting Kit-8 assays revealed that the downregulation of TFAP2A reduced the growth rate. (C) Colony formation assay revealed that the downregulation of TFAP2A reduced the growth rate. (D) Apoptosis detection using flow cytometric analysis revealed that downregulation of TFAP2A promoted the apoptotic rate. (E) Transwell assay revealed that the downregulation of TFAP2A reduced the migration and invasion rate. n=3 in each group. \*P<0.05, \*\*P<0.01 and \*\*\*P<0.001. TFAP2A, transcription factor AP-2 alpha; sh-, short hairpin.

In addition, the expression of TFAP2A and PD-L1 was examined in three cervical cancer cell lines and cervical epithelial cells. It was found that TFAP2A and PD-L1 expression was higher in the HeLa and SiHa cervical cancer cell lines than in the END1 cells (Fig. 2D and E). To further validate the association between TFAP2A and PD-L1 in cervical cancer, TFAP2A was

stably knocked down and overexpressed in HeLa and SiHa cells using lentiviral transfection. Notably, the protein level of PD-L1 was significantly increased following TFAP2A overexpression (Fig. 2F), whereas the protein level of PD-L1 was significantly decreased following TFAP2A knockdown (Fig. 2G), indicating that TFAP2A positively regulated PD-L1 expression.

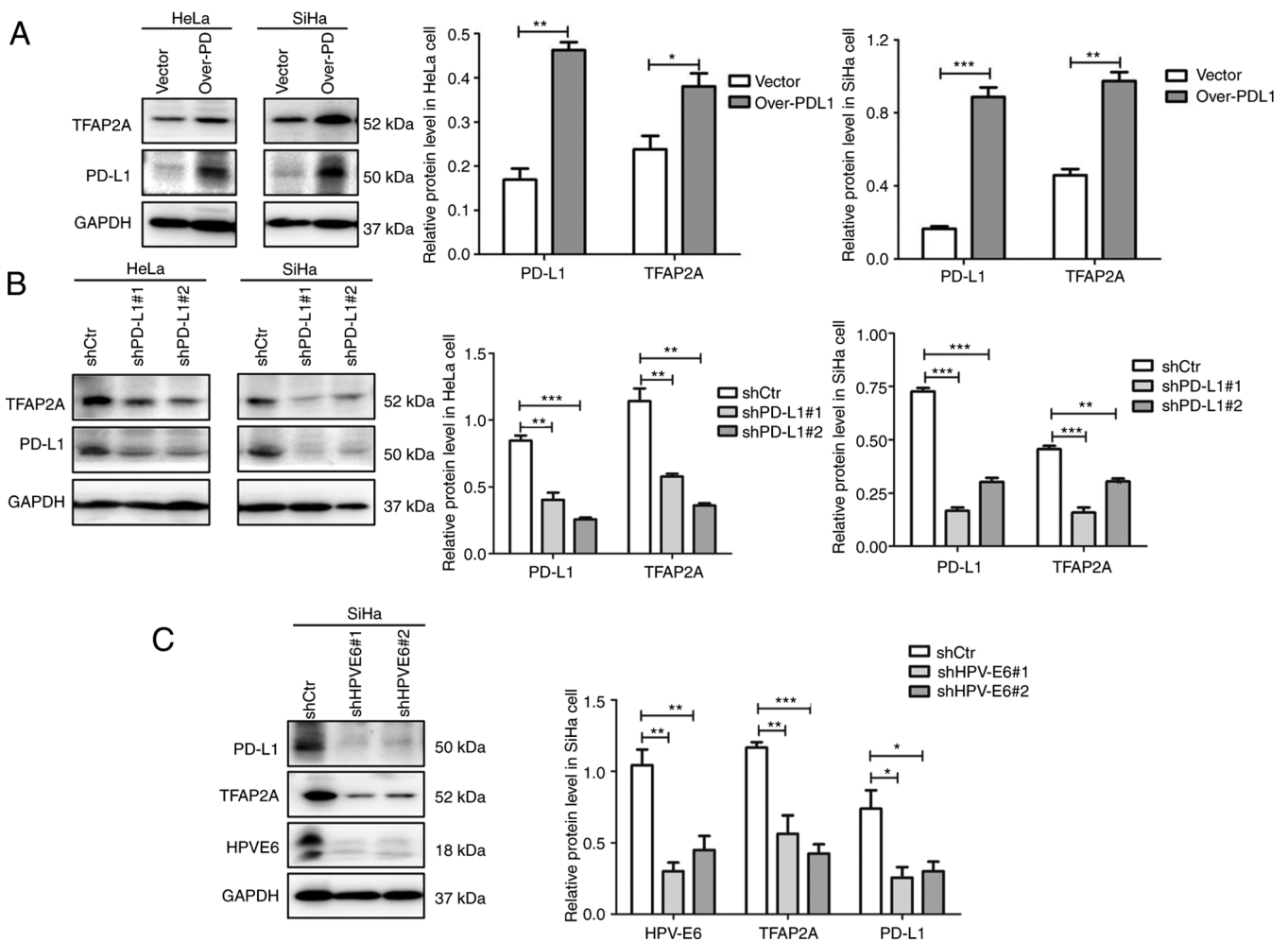


Figure 4. TFAP2A and PD-L1 form a positive feedback pathway, which may be regulated by HPV E6 protein. (A) Western blot analysis revealed that TFAP2A expression was reduced in PD-L1-overexpressing cervical cancer cell lines. (B) Western blot analysis revealed that TFAP2A expression was reduced in cervical cancer cell lines in which PD-L1 was knocked down. (C) Western blot analysis revealed that TFAP2A and PD-L1 expression was reduced in cervical cancer cells in which HPV E6 was knocked down.  $n=3$  in each group. \* $P<0.05$ , \*\* $P<0.01$  and \*\*\* $P<0.001$ . TFAP2A, transcription factor AP-2 alpha; PD-L1, programmed death-ligand 1; sh-, short hairpin.

*TFAP2A knockdown inhibits cervical cancer cell proliferation, migration and invasion, and promotes apoptosis.* In HeLa and SiHa cells in which TFAP2A was knocked down, the role of TFAP2A in cervical cancer was investigated. As shown by the results of wound healing assay, cell migration was significantly reduced following TFAP2A knockdown (Fig. 3A). Cell proliferation and colony formation were also inhibited after TFAP2A knockdown (Fig. 3B and C). Furthermore, TFAP2A knockdown increased apoptosis (Fig. 3D). Of note, TFAP2A knockdown inhibited cell migration and invasion (Fig. 3E). These findings indicated that tumor metastasis was reduced and apoptosis was promoted following TFAP2A knockdown. These findings indicated that TFAP2A has potential oncogenic properties.

*TFAP2A and PD-L1 form a positive feedback loop that may be influenced by the HPV E6 protein.* To further investigate the association between TFAP2A and PD-L1, PD-L1 was overexpressed and knocked down in the HeLa and SiHa cervical cancer cell lines using plasmid transfection. Notably, it was found that the overexpression of PD-L1 resulted in an elevated protein level of TFAP2A (Fig. 4A),

whereas the knockdown of PD-L1 resulted in a decrease in its expression (Fig. 4B). Such consistent changes suggest that TFAP2A and PD-L1 regulate each other, forming a positive feedback loop. The results based on Table I suggested that TFAP2A expression is linked to HPV infection. In the present study, HPV 16 E6 was knocked down in SiHa cells to further investigate this link. The results revealed that the knockdown of E6 protein led to a significant decrease in TFAP2A and PD-L1 protein expression (Fig. 4C), suggesting that HPV E6 protein regulates TFAP2A and PD-L1 protein expression. A positive feedback regulates TFAP2A and PD-L1, according to these findings. HPV E6 protein may upregulate TFAP2A expression, resulting in an increased PD-L1 protein expression.

*TFAP2A promotes the proliferation and migration, and inhibits the apoptosis of cervical cancer cells via PD-L1.* To investigate the functional axis between TFAP2A and PD-L1 in cervical cancer, sh-TFAP2A stable cell lines were generated using the SiHa and HeLa cells, which were then transiently transfected with a PD-L1 overexpression plasmid (sh-TFAP2A#1 + PD-L1). The results of western blot analysis



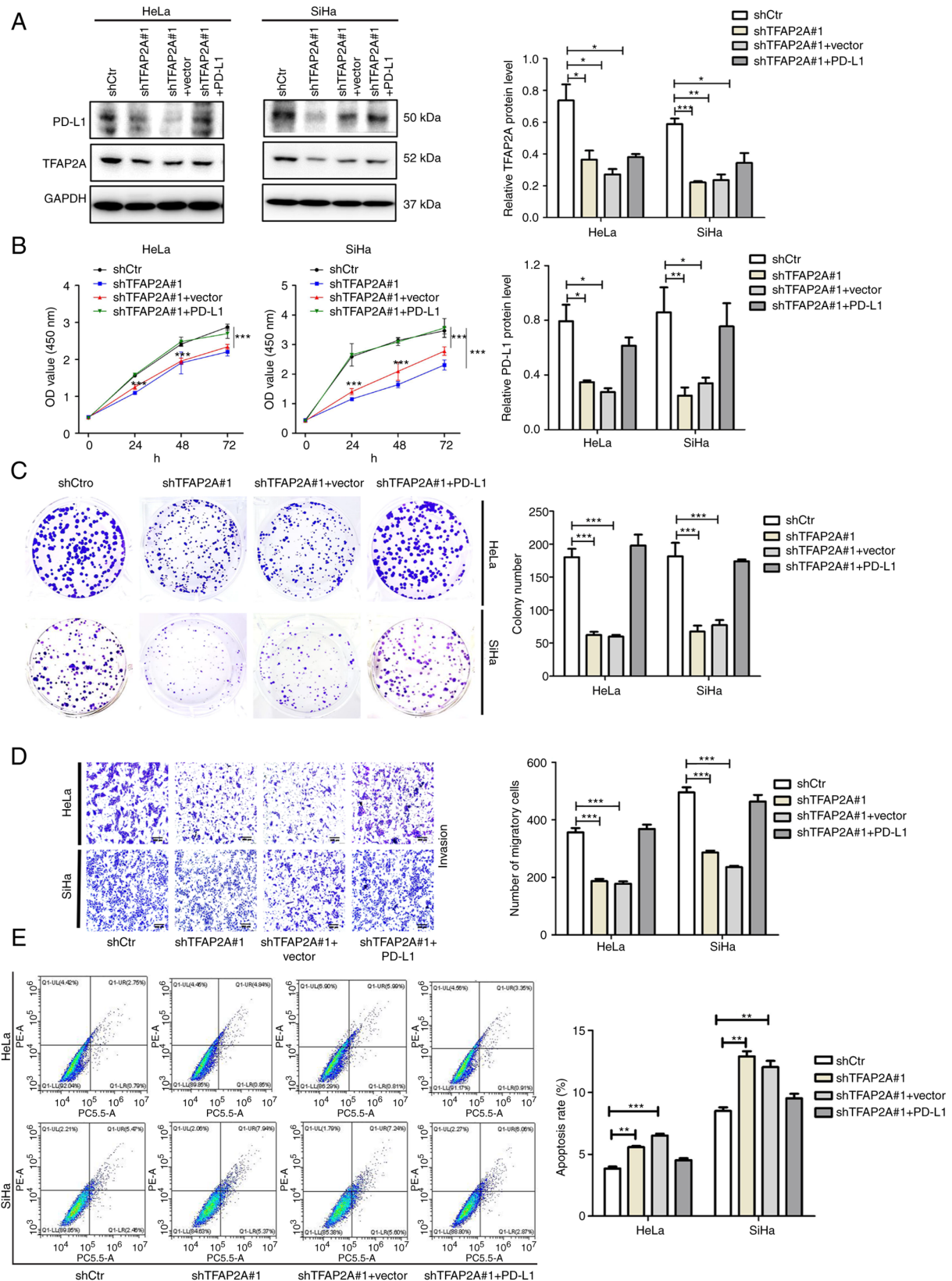


Figure 5. TFAP2A promotes the proliferation and migration, and inhibits the apoptosis of cervical cancer cells via PD-L1. (A) Western blot analysis of TFAP2A, PD-L1 expression in the shctr, shTFAP2A#1, shTFAP2A #1 + Vector and shTFAP2A #1 + PD-L1 groups. (B) Cell Counting Kit-8 assays revealed the growth rate of the cells. (C) Colony formation assay revealed the proliferation of the cells. (D) Transwell assay revealed the migration and invasion of cells. (E) Apoptosis detection using flow cytometric analysis revealed apoptosis rate of the cells. n=3 in each group. \*P<0.05, \*\*P<0.01 and \*\*\*P<0.001. TFAP2A, transcription factor AP-2 alpha; PD-L1, programmed death-ligand 1; sh-, short hairpin.

revealed that the expression of PD-L1 was also significantly decreased following the knockdown of TFAP2A, and the

expression of PD-L1 was partially restored following the overexpression of PD-L1 in the sh-TFAP2A group (Fig. 5A).



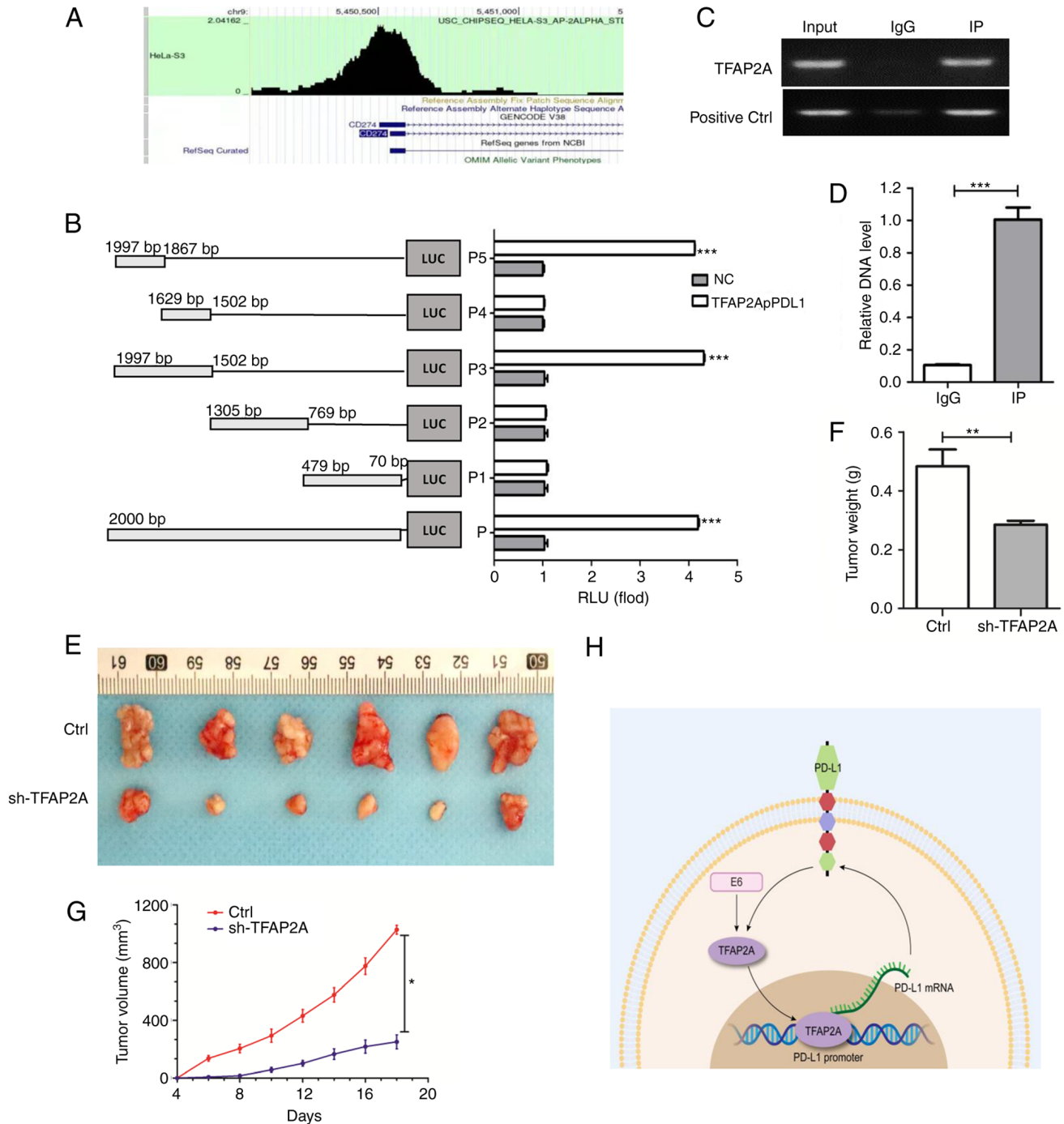


Figure 6. TFAP2A targets PD-L1 and the knockdown of TFAP2A inhibits the progression of cervical cancer. (A) Enrichment of TFAP2A in the PD-L1 promoter region in RNA-Seq Atlas [RNA-Seq Atlas-Database Commons (cnb.ac.cn)]. (B) PD-L1 promoter transient reporter assay, including deletions of the putative binding sites. Results are represented as normalized RLUs. (C and D) Chromatin Immunoprecipitation assay was used to determine the physical interaction of TFAP2A protein with the -PD-L1 promoter region and reverse transcription-quantitative PCR was used to analyze immune complexes. (E) Gross images of excised tumors in the control, Ctrl, sh-TFAP2A groups. (F) Tumor volume and (G) tumor weight. (H) Experimental hypothesis diagram; n=6 in each group. \*P<0.05, \*\*P<0.01 and \*\*\*P<0.001. TFAP2A, transcription factor AP-2 alpha; PD-L1, programmed death-ligand 1; RLUs, relative luciferase units; sh-, short hairpin.

In the sh-TFAP2A#1 + PD-L1 group, cell proliferation was increased (Fig. 5B), colony formation was restored (Fig. 5C) and cell migration was also significantly promoted (Fig. 5D) compared with the sh-TFAP2A#1 + Vector group. At the same time, the proportion of apoptotic cells decreased (Fig. 5E). These results demonstrated that TFAP2A relies on the PD-L1 pathway to regulate the proliferation, migration and apoptosis of cervical cancer cells.

*TFAP2A suppresses the progression of cervical cancer by targeting PD-L1.* TFAP2A and PD-L1 are closely related and regulate each other. Herein, to investigate the binding between them, the enrichment of TFAP2A in the PD-L1 promoter region was first predicted using bioinformatics (Fig. 6A). A subsequent dual luciferase reporter gene assay (Fig. 6B) confirmed that a TFAP2A binding site was located in the PD-L1 promoter region. RT-qPCR was also used to examine

the immune complexes. The findings revealed that TFAP2A physically interacted with PD-L1 protein (Fig. 6C and D). Finally, to improve the understanding of the role of TFAP2A in the development of cervical cancer *in vivo*, a mouse cervical cancer transplantation tumor model was generated using HeLa cells. The results revealed that the group subjected to knockdown TFAP2A exhibited a slower tumor growth and a significantly lower final tumor weight and volume (Fig. 6E-G). TFAP2A knockdown significantly inhibited the growth of HeLa-derived tumors *in vivo*. On the whole, it was found that TFAP2A can promote the transcription of PD-L1 promoter by binding to it and affect the expression of HPV 16 E6, thus promoting the progression of cervical cancer (Fig. 6H).

## Discussion

In the present study, it was found that TFAP2A was highly expressed in cervical cancer tissues and cells, and was associated with a more advanced tumor stage and distant metastasis. The silencing of TFAP2A expression significantly inhibited the proliferation and migration of cervical cancer cells, and promoted apoptosis. A mouse xenograft tumor model was used to confirm the tumor-promoting function of TFAP2A. In addition, it was found that TFAP2A directly targeted PD-L1 to promote cervical cancer cell growth, and HPV E6 may be a potential influencing factor of this pathway.

The transcription factor TFAP2A, a AP-2 family member, has been demonstrated to be involved in essential life processes, including embryonic ectodermal development, stem cell differentiation and cell growth and proliferation (24). The role of TFAP2A in carcinogenesis and development has only recently been recognized. It is highly expressed in a variety of cancer types, including bladder cancer, melanoma, head and neck squamous carcinoma (25), gastric cancer (6), ovarian cancer (9), lung adenocarcinoma (7) and nasopharyngeal carcinoma (8). The overexpression of TFAP2A predicts a very poor prognosis. In head and neck squamous carcinoma, TFAP2A downregulation has been shown to be associated with a reduced proliferation (26,27). The high expression of TFAP2A promotes cancer cell proliferation and inhibits apoptosis (13). In nasopharyngeal carcinoma, TFAP2A overexpression has been shown to be positively associated with tumor stage, local infiltration and a decreased overall survival, and TFAP2 silencing results in a slower proliferation of cancer cells (8). The silencing of TFAP2A has been shown to inhibit the proliferation, migration and invasiveness of esophageal cancer cells, and to enhance apoptosis (28). The increased expression of TFAP2A has been demonstrated in gallbladder cancer, and its inhibition reduces the proliferation, migration and invasion of gallbladder cancer cells (29). However, TFAP2A has been revealed to be a tumor suppressor and to be expressed in low levels in a few malignancies, including hepatocellular carcinoma, glioma and colon cancer (30). This suggests that TFAP2A has a dual identity and can serve as an oncogene or tumor suppressor gene, depending on the tumor type. As a result, the present study aimed to examine its expression profile in cervical cancer. It was identified that TFAP2A was highly expressed in cervical cancer and was associated with tumor stage and lymph node metastasis. It should be noted that due to the extremely low incidence of

cervical adenocarcinoma (2), the present study mainly focused on squamous carcinoma of the cervix. More than 80% of the selected public data sets and follow-up clinical specimens were also cervical squamous carcinoma, and the selected cell line SiHa was also derived from squamous carcinoma of the cervix (31). In addition, it was confirmed that TFAP2A knockdown inhibited the proliferation, invasion and migration of cervical cancer cells, while promoting apoptosis, indicating oncogenic potential.

TFAP2A was found to act as a transcription factor to regulate the level and activity of downstream signaling proteins, acting in various cancers or different types of cell lines by activating different signaling pathways. For example, in melanoma, TFAP2 promotes tumor metastasis by activating the Enhancer of Zeste Homolog 2 (EZH2). Gene (25). TFAP2A promotes the growth and survival of nasopharyngeal carcinoma by targeting the HIF-1 and VEGF pathways in nasopharyngeal carcinoma cells (8). In lung cancer, TFAP2A directly upregulates BMP4 to promote angiogenesis and lead to acquired resistance to anlotinib (32). TFAP2A activates heme oxygenase-1 (HO-1) to promote tumor growth (15), upregulates telomerase to resist apoptosis (33), induces Keratin 16 (KRT16) and Inositol-Trisphosphate 3-Kinase A (ITPKA) overexpression, and promotes lung cancer tumorigenicity through epithelial-mesenchymal transition (7,11). In addition, several studies have found that certain long non-coding RNAs or microRNAs (miRs) regulate the post-transcriptional levels of TFAP2A which affect the biological functions of tumors. For example, Linc00467 can regulate miR-1285-3p/TFAP2A expression, thereby facilitating the invasion of head and neck squamous cell carcinoma cells and inhibiting apoptosis (13). Long-stranded non-coding RNA TFAP2A-AS1 produces oncogenic effects in oral squamous cell carcinoma by regulating the miR-1297/TFAP2A axis (34). miR-876-5p inhibits breast cancer progression by regulating cell proliferation, migration and invasion in a TFAP2A-dependent manner (35). TFAP2A enhances lung adenocarcinoma metastasis via miR-16 family/TFAP2A/PSG9/TGF- $\beta$  signaling pathway (12). Silencing of lymphocytic leukemia deletion gene1 (DLEU1) inhibited ovarian cancer cell proliferation, migration and invasion by regulating the miR-429/TFAP2A axis (9). Zinc-finger protein 471 (ZNF471) acts as a tumor suppressor in gastric cancer by transcriptionally repressing the downstream targets TFAP2A and Plastin 3 (PLS3) (6). Of note, the present study found that TFAP2A interacted directly with PD-L1 and produced a hitherto unknown positive feedback signaling loop in cervical cancer.

PD-L1 is an immunosuppressive signaling protein that induces tumor immune escape (36). Previous studies have examined the expression of PD-L1 in cervical cancer and have reported that PD-L1 is more commonly expressed in cervical cancer than in normal cervical tissues, ranging from 34.4-96% (37,38). PD-L1 expression has been observed to be more widespread in cervical squamous cell carcinoma, with a percentage of tissue-positive samples exceeding 37% (39,40). These findings demonstrated that PD-L1 is widely expressed in cervical cancer tumor cells. These results support prior results regarding the elevated expression of PD-L1 in cervical cancer. Furthermore, PD-L1 protein is substantially connected with cervical cancer prognosis, with a higher PD-L1 expression

being positively associated with tumor metastasis (41), tumor progression (42) and a poor prognosis of patients with cervical cancer (43). In the present study, TFAP2A was found to promote the proliferation and migration of cervical cancer cells through PD-L1, while inhibiting cell apoptosis. However, certain researchers have concluded that PD-L1 expression is not associated with progression-free or overall survival in patients with cervical cancer (37), and that borderline PD-L1 expression is associated with an improved prognosis than diffuse PD-L1 expression or no PD-L1 expression (44). The explanation for the contradictory prior research may be due to the degree and pattern of PD-L1 expression, in addition to the diverse tissue subtypes with varied PD-L1 expression and function, which can influence the different prognoses of cervical cancer.

The regulatory mechanisms of PD-L1 expression in malignancies are complex and diverse, including genomic abnormalities, transcriptional control, mRNA stability, oncogenic signaling and protein stability (21). The current study demonstrated that TFAP2A promoted the expression of PD-L1 by binding to the promoter region of PD-L1, and its binding site was 1876-1997 bp in the PD-L1 promoter region. But how TFAP2A upregulate PD-L1 remains unknown. Earlier studies have found that the C-terminal region of AP-2 family proteins contains a helix-turn-helix domain that mediates dimerization and site-specific DNA sequence GCCNNGGC binding, thereby inducing transcriptional activation (45). It has also been confirmed that the activator of human AP-2 $\alpha$  is located in amino acids 52-108 (46). In other words, TFAP2A may activate PD-L1 transcription by specifically recognizing and binding to the GCCNNGGC sequence in the 1876-1997 bp region of the PD-L1 promoter. In addition, the transcription process of PD-L1 in the nucleus is also very complex. Studies have found that under hypoxia (47), p-Stat3 physically interacts with PD-L1 to promote its nuclear translocation. Another study reported that PD-L1 in the nucleus further regulates Gas6 expression and activates the MerTK signaling pathway to promote proliferation of NSCLC cells (48).

In addition, it was also identified that PD-L1 can affect the expression of TFAP2A. However, there are no relevant studies on how PD-L1 affects TFAP2A, but studies have found the intrinsic function of PD-L1 in tumors and its interaction with other carcinogenic pathways. The high expression of PD-L1 interacts with mTOR signaling pathway to promote the growth and autophagy of ovarian cancer cells and melanoma cells (49). PD-L1 binds to ITGB4 in cervical cancer (50), triggering AKT/GSK3 $\beta$  and SNAI1/SIRT3 signaling pathways. PD-L1/ITGB6/STAT3 signaling axis regulates bladder cancer cell proliferation, glucose metabolism and chemotherapy resistance (51). PD-L1 regulates the proliferation and apoptosis of AML cell lines through the PI3K/AKT signaling pathway (52). However, PI3K-AKT pathway can affect the expression of TFAP2A (53), suggesting that PI3K-AKT pathway may be a key mediator in PD-L1 regulation of TFAP2A, which is interesting and worthy of further exploration.

Finally, the signaling upstream of TFAP2A was actively investigated and it was identified that the oncogenic protein HPV E6 may be a potential factor in regulating the TFAP2A/PD-L1 signaling pathway. Studies have found that the PD-L1 expression was linked to promoting HPV-induced cervical carcinogenesis. The HPV E5/E6/E7 oncogene

stimulates numerous signaling pathways, including PI3K/AKT, MAPK, hypoxia-inducible factor 1, STAT3/NF- $\kappa$ B and microRNAs, which regulate the PD-L1/PD-1 axis (54). It has also been reported that the AP-2 transcription factor family, in which TFAP2A is located, was found to have binding sites in the transcriptional control region (upstream regulatory region, URR) of several HPV types (55-58), including HPV11 and HPV18, suggesting that AP-2 may be a key activator of viral E6/E7 oncogene expression, but it was further found to have only a slight effect on the activity of the E6/E7 oncogene promoter (59). Suggesting that AP-2 itself is not critical for the E6/E7 promoter, it is also possible that additional AP-2 binding sites may be present in the viral URRs and affect the activity of the E6/E7 promoter, as AP-2 is an epithelial transcription factor and therefore may contribute to the preferential transcriptional activity of HPV URRs. However, there is no study on the functional significance of TFAP2A on HPV E6/E7. The present study found a potential association between TFAP2A and E6, and also provided a little idea about the regulatory mechanism of E6 in cervical cancer.

In conclusion, the present study demonstrated the high expression profile of TFAP2A in cervical cancer and that it is associated with a poorer prognosis. TFAP2A plays a key role in promoting cervical cancer progression by directly interacting with PD-L1. Thus, the present study revealed a possible molecular mechanism of TFAP2A in cervical cancer. The inhibition of TFAP2A may therefore provide some theoretical basis for the treatment of patients with cervical cancer.

## Acknowledgements

Not applicable.

## Funding

The present study was supported by the National Natural Science Foundation of China (grant no. 8197103302).

## Availability of data and materials

The datasets used and/or analyzed during the current study are available from the corresponding author upon reasonable request.

## Authors' contributions

JY and YG designed the experiments. JY and SW mainly conducted cell experiments. YG and SW undertook all animal experiments. JY, YG, SY and HC collated and analyzed the data. JY, HC and SY drafted the manuscript. YG and HC performed language correction. JY and YG confirm the authenticity of all the raw data. All authors have read and approved the final manuscript.

## Ethics approval and consent to participate

All procedures regarding human tissue studies were approved (approval no. 2022120K) by the Ethical board of Zhongnan Hospital of Wuhan University (Wuhan, China). The waiver of informed consent has been approved by the ethics Committee.

The animal experiments were performed according to the Animal Care and Use Committee guidelines at the Zhongnan Hospital of Wuhan University (approval no. ZN2021257).

### Patient consent for publication

Not applicable.

### Competing interests

The authors declare that they have no competing interests.

### References

- Martínez-Rodríguez F, Limones-González JE, Mendoza-Almanza B, Esparza-Ibarra EL, Gallegos-Flores PI, Ayala-Luján JL, Ayala-Luján JL, Godina-González S, Salinas E and Mendoza-Almanza G: Understanding cervical cancer through proteomics. *Cells* 10: 1854, 2021.
- Revathidevi S, Murugan AK, Nakaoka H, Inoue I and Munirajan AK: APOBEC: A molecular driver in cervical cancer pathogenesis. *Cancer Lett* 496: 104-116, 2021.
- Sung H, Ferlay J, Siegel RL, Laversanne M, Soerjomataram I, Jemal A and Bray F: Global Cancer Statistics 2020: GLOBOCAN estimates of incidence and mortality worldwide for 36 cancers in 185 countries. *CA Cancer J Clin* 71: 209-249, 2021.
- Yamashita H, Kawasaki YI, Shuman L, Zheng Z, Tran T, Walter V, Warrick JJ, Chen G, Al-Ahmadie H, Kaag M, *et al*: Repression of transcription factor AP-2 alpha by PPAR $\gamma$  reveals a novel transcriptional circuit in basal-squamous bladder cancer. *Oncogenesis* 8: 69, 2019.
- Wu J: Pancreatic cancer-derived exosomes promote the proliferation, invasion, and metastasis of pancreatic cancer by the miR-3960/TFAP2A Axis. *J Oncol* 2022: 3590326, 2022.
- Cao L, Wang S, Zhang Y, Wong KC, Nakatsu G, Wang X, Wong S, Ji J and Yu J: Zinc-finger protein 471 suppresses gastric cancer through transcriptionally repressing downstream oncogenic PLS3 and TFAP2A. *Oncogene* 37: 3601-3616, 2018.
- Guoren Z, Zhaohui F, Wei Z, Mei W, Yuan W, Lin S, Xiaoyue X, Xiaomei Z and Bo S: TFAP2A Induced ITPKA Serves as an oncogene and interacts with DBN1 in lung adenocarcinoma. *Int J Biol Sci* 16: 504-514, 2020.
- Shi D, Xie F, Zhang Y, Tian Y, Chen W, Fu L, Wang J, Wang W, Kang T, Huang W and Deng W: TFAP2A regulates nasopharyngeal carcinoma growth and survival by targeting HIF-1 $\alpha$  signaling pathway. *Cancer Prev Res (Phila)* 7: 266-277, 2014.
- Xu H, Wang L and Jiang X: Silencing of lncRNA DLEU1 inhibits tumorigenesis of ovarian cancer via regulating miR-429/TFAP2A axis. *Mol Cell Biochem* 476: 1051-1061, 2021.
- Chen S, Li H, Li X, Chen W, Zhang X, Yang Z, Chen Z, Chen J, Zhang Y, Shi D and Song M: High SOX8 expression promotes tumor growth and predicts poor prognosis through GOLPH3 signaling in tongue squamous cell carcinoma. *Cancer Med* 9: 4274-4289, 2020.
- Yuanhua L, Pudong Q, Wei Z, Yuan W, Delin L, Yan Z, Geyu L and Bo S: TFAP2A Induced KRT16 as an oncogene in lung adenocarcinoma via EMT. *Int J Biol Sci* 15: 1419-1428, 2019.
- Xiong Y, Feng Y, Zhao J, Lei J, Qiao T, Zhou Y, Lu Q, Jiang T, Jia L and Han Y: TFAP2A potentiates lung adenocarcinoma metastasis by a novel miR-16 family/TFAP2A/PSG9/TGF- $\beta$  signaling pathway. *Cell Death Dis* 12: 352, 2021.
- Liang Y, Cheng G, Huang D and Yuan F: Linc00467 promotes invasion and inhibits apoptosis of head and neck squamous cell carcinoma by regulating miR-1285-3p/TFAP2A. *Am J Transl Res* 13: 6248-6259, 2021.
- Hao H, Xiao D, Pan J, Qu J, Egger M, Waigel S, Sanders MA, Zacharias W, Rai SN and McMasters KM: Sentinel lymph node genes to predict prognosis in node-positive melanoma patients. *Ann Surg Oncol* 24: 108-116, 2017.
- Pu M, Li C, Qi X, Chen J, Wang Y, Gao L, Miao L and Ren J: MiR-1254 suppresses HO-1 expression through seed region-dependent silencing and non-seed interaction with TFAP2A transcript to attenuate NSCLC growth. *PLoS Genet* 13: e1006896, 2017.
- Brody R, Zhang Y, Ballas M, Siddiqui MK, Gupta P, Barker C, Midha A and Walker J: PD-L1 expression in advanced NSCLC: Insights into risk stratification and treatment selection from a systematic literature review. *Lung Cancer* 112: 200-215, 2017.
- Jiang Y, Chen M, Nie H and Yuan Y: PD-1 and PD-L1 in cancer immunotherapy: Clinical implications and future considerations. *Hum Vaccin Immunother* 15: 1111-1122, 2019.
- Wei F, Zhang T, Deng SC, Wei JC, Yang P, Wang Q, Chen ZP, Li WL, Chen HC, Hu H and Cao J: PD-L1 promotes colorectal cancer stem cell expansion by activating HMGA1-dependent signaling pathways. *Cancer Lett* 450: 1-13, 2019.
- Darvin P, Toor SM, Sasidharan Nair V and Elkord E: Immune checkpoint inhibitors: Recent progress and potential biomarkers. *Exp Mol Med* 50: 1-11, 2018.
- Frenel JS, Le Tourneau C, O'Neil B, Ott PA, Piha-Paul SA, Gomez-Roca C, van Brummelen EMJ, Rugo HS, Thomas S, Saraf S, *et al*: Safety and efficacy of pembrolizumab in advanced, programmed death ligand 1-positive cervical cancer: Results From the Phase Ib KEYNOTE-028 Trial. *J Clin Oncol* 35: 4035-4041, 2017.
- Sun C, Mezzadra R and Schumacher TN: Regulation and Function of the PD-L1 Checkpoint. *Immunity* 48: 434-452, 2018.
- Livak KJ and Schmittgen TD: Analysis of relative gene expression data using real-time quantitative PCR and the 2(-Delta Delta C(T)) Method. *Methods* 25: 402-408, 2001.
- Orso F, Corà D, Ubezio B, Provero P, Caselle M and Taverna D: Identification of functional TFAP2A and SP1 binding sites in new TFAP2A-modulated genes. *BMC Genomics* 11: 355, 2010.
- Tchieu J, Zimmer B, Fattahi F, Amin S, Zeltner N, Chen S and Studer L: A modular platform for differentiation of human PSCs into all major ectodermal lineages. *Cell Stem Cell* 21: 399-410. e7, 2017.
- White JR, Thompson DT, Koch KE, Kiriazov BS, Beck AC, van der Heide DM, Grimm BG, Kulak MV and Weigel RJ: AP-2 $\alpha$ -Mediated Activation of E2F and EZH2 drives melanoma metastasis. *Cancer Res* 81: 4455-4470, 2021.
- Bennett KL, Romigh T and Eng C: AP-2alpha induces epigenetic silencing of tumor suppressive genes and microsatellite instability in head and neck squamous cell carcinoma. *PLoS One* 4: e6931, 2009.
- Kagohara LT, Zamuner F, Davis-Marcisak EF, Sharma G, Considine M, Allen J, Yegnasubramanian S, Gaykalova DA and Fertig EJ: Integrated single-cell and bulk gene expression and ATAC-seq reveals heterogeneity and early changes in pathways associated with resistance to cetuximab in HNSCC-sensitive cell lines. *Br J Cancer* 123: 101-113, 2020.
- Zhu JL, Xue WB, Jiang ZB, Feng W, Liu YC, Nie XY and Jin LY: Long noncoding RNA CDKN2B-AS1 silencing protects against esophageal cancer cell invasion and migration by inactivating the TFAP2A/FSCN1 axis. *Kaohsiung J Med Sci* 38: 1144-1154, 2022.
- Huang HX, Yang G, Yang Y, Yan J, Tang XY and Pan Q: TFAP2A is a novel regulator that modulates ferroptosis in gallbladder carcinoma cells via the Nrf2 signalling axis. *Eur Rev Med Pharmacol Sci* 24: 4745-4755, 2020.
- Kołat D, Kałuzińska Z, Bednarek AK and Pluciennik E: The biological characteristics of transcription factors AP-2 $\alpha$  and AP-2 $\gamma$  and their importance in various types of cancers. *Biosci Rep* 39: BSR20181928, 2019.
- Fan L, Liu Z, Zhang Y, Zhu H, Yu H, Yang F, Yang R and Wu F: MiRNA373 induces cervical squamous cell carcinoma SiHa cell apoptosis. *Cancer Biomark* 21: 455-460, 2018.
- Zhang LI, Lu J, Liu RQ, Hu MJ, Zhao YM, Tan S, Wang SY, Zhang B, Nie W, Dong Y, *et al*: Chromatin accessibility analysis reveals that TFAP2A promotes angiogenesis in acquired resistance to anlotinib in lung cancer cells. *Acta Pharmacol Sin* 41: 1357-1365, 2020.
- Wei CW, Lin CC, Yu YL, Lin CY, Lin PC, Wu MT, Chen CJ, Chang W, Lin SZ, Chen YL and Harn HJ: n-Butylidenephthalide induced apoptosis in the A549 human lung adenocarcinoma cell line by coupled down-regulation of AP-2alpha and telomerase activity. *Acta Pharmacol Sin* 30: 1297-1306, 2009.
- Yang K, Niu Y, Cui Z, Jin L, Peng S and Dong Z: Long noncoding RNA TFAP2A-AS1 promotes oral squamous cell carcinoma cell growth and movement via competitively binding miR-1297 and regulating TFAP2A expression. *Mol Carcinog* 61: 865-875, 2022.
- Xu J, Zheng J, Wang J and Shao J: miR-876-5p suppresses breast cancer progression through targeting TFAP2A. *Exp Ther Med* 18: 1458-1464, 2019.



36. Kluger HM, Zito CR, Turcu G, Baine MK, Zhang H, Adeniran A, Sznol M, Rimm DL, Kluger Y, Chen L, *et al*: PD-L1 studies across tumor types, its differential expression and predictive value in patients treated with immune checkpoint inhibitors. *Clin Cancer Res* 23: 4270-4279, 2017.
37. Enwere EK, Kornaga EN, Dean M, Koulis TA, Phan T, Kalantarian M, Köbel M, Ghatage P, Magliocco AM, Lees-Miller SP and Doll CM: Expression of PD-L1 and presence of CD8-positive T cells in pre-treatment specimens of locally advanced cervical cancer. *Mod Pathol* 30: 577-586, 2017.
38. Meng Y, Liang H, Hu J, Liu S, Hao X, Wong MSK, Li X and Hu L: PD-L1 expression correlates with tumor infiltrating lymphocytes and response to neoadjuvant chemotherapy in cervical cancer. *J Cancer* 9: 2938-2945, 2018.
39. Mezache L, Paniccia B, Nyinawabera A and Nuovo GJ: Enhanced expression of PD L1 in cervical intraepithelial neoplasia and cervical cancers. *Mod Pathol* 28: 1594-1602, 2015.
40. Huang RSP, Haberberger J, Murugesan K, Danziger N, Hiemenz M, Severson E, Duncan DL, Ramkissoon SH, Ross JS, Elvin JA and Lin DI: Clinicopathologic and genomic characterization of PD-L1-positive uterine cervical carcinoma. *Mod Pathol* 34: 1425-1433, 2021.
41. Yang W, Lu YP, Yang YZ, Kang JR, Jin YD and Wang HW: Expressions of programmed death (PD)-1 and PD-1 ligand (PD-L1) in cervical intraepithelial neoplasia and cervical squamous cell carcinomas are of prognostic value and associated with human papillomavirus status. *J Obstet Gynaecol Res* 43: 1602-1612, 2017.
42. Hsu PC, Li SH and Yang CT: Recurrent Pneumonitis Induced by Atezolizumab (Anti-Programmed Death Ligand 1) in NSCLC patients who previously experienced anti-programmed death 1 immunotherapy-related pneumonitis. *J Thorac Oncol* 13: e227-e230, 2018.
43. Heeren AM, Punt S, Bleeker MC, Gaarenstroom KN, van der Velden J, Kenter GG, de Gruijl TD and Jordanova ES: Prognostic effect of different PD-L1 expression patterns in squamous cell carcinoma and adenocarcinoma of the cervix. *Mod Pathol* 29: 753-763, 2016.
44. Karim R, Jordanova ES, Piersma SJ, Kenter GG, Chen L, Boer JM, Melief CJ and van der Burg SH: Tumor-expressed B7-H1 and B7-DC in relation to PD-1+ T-cell infiltration and survival of patients with cervical carcinoma. *Clin Cancer Res* 15: 6341-6347, 2009.
45. Lambert SA, Jolma A, Campitelli LF, Das PK, Yin Y, Albu M, Chen X, Taipale J, Hughes TR and Weirauch MT: The human transcription factors. *Cell* 172: 650-665, 2018.
46. Wankhade S, Yu Y, Weinberg J, Tainsky MA and Kannan P: Characterization of the activation domains of AP-2 family transcription factors. *J Biol Chem* 275: 29701-29708, 2000.
47. Hou J, Zhao R, Xia W, Chang CW, You Y, Hsu JM, Nie L, Chen Y, Wang YC, Liu C, *et al*: PD-L1-mediated gasdermin C expression switches apoptosis to pyroptosis in cancer cells and facilitates tumour necrosis. *Nat Cell Biol* 22: 1264-1275, 2020.
48. Du W, Zhu J, Zeng Y, Liu T, Zhang Y, Cai T, Fu Y, Zhang W, Zhang R, Liu Z and Huang JA: KPNB1-mediated nuclear translocation of PD-L1 promotes non-small cell lung cancer cell proliferation via the Gas6/MerTK signaling pathway. *Cell Death Differ* 28: 1284-1300, 2021.
49. Clark CA, Gupta HB, Sareddy G, Pandeswara S, Lao S, Yuan B, Drerup JM, Padron A, Conejo-Garcia J, Murthy K, *et al*: Tumor-Intrinsic PD-L1 Signals Regulate Cell Growth, Pathogenesis, and Autophagy in Ovarian Cancer and Melanoma. *Cancer Res* 76: 6964-6974, 2016.
50. Wang S, Li J, Xie J, Liu F, Duan Y, Wu Y, Huang S, He X, Wang Z and Wu X: Programmed death ligand 1 promotes lymph node metastasis and glucose metabolism in cervical cancer by activating integrin  $\beta$ 4/SNAI1/SIRT3 signaling pathway. *Oncogene* 37: 4164-4180, 2018.
51. Cao D, Qi Z, Pang Y, Li H, Xie H, Wu J, Huang Y, Zhu Y, Shen Y, Zhu Y, *et al*: Retinoic acid-related orphan receptor C regulates proliferation, glycolysis, and chemoresistance via the PD-L1/ITGB6/STAT3 signaling axis in bladder cancer. *Cancer Res* 79: 2604-2618, 2019.
52. Wang F, Yang L, Xiao M, Zhang Z, Shen J, Anuchapreeda S, Tima S, Chiampanichayakul S and Xiao Z: PD-L1 regulates cell proliferation and apoptosis in acute myeloid leukemia by activating PI3K-AKT signaling pathway. *Sci Rep* 12: 11444, 2022.
53. Beck AC, Cho E, White JR, Paemka L, Li T, Gu VW, Thompson DT, Koch KE, Franke C, Gosse M, *et al*: AP-2 $\alpha$  Regulates S-Phase and is a marker for sensitivity to PI3K inhibitor buparlisib in colon cancer. *Mol Cancer Res* 19: 1156-1167, 2021.
54. Zhang L, Zhao Y, Tu Q, Xue X, Zhu X and Zhao KN: The roles of programmed cell death ligand-1/programmed cell death-1 (PD-L1/PD-1) in HPV-induced cervical cancer and potential for their use in blockade therapy. *Curr Med Chem* 28: 893-909, 2021.
55. Royer HD, Freyaldenhoven MP, Napierski I, Spitkovsky DD, Bauknecht T and Dathan N: Delineation of human papillomavirus type 18 enhancer binding proteins: The intracellular distribution of a novel octamer binding protein p92 is cell cycle regulated. *Nucleic Acids Res* 19: 2363-2371, 1991.
56. Turek LP: The structure, function, and regulation of papilloma-viral genes in infection and cervical cancer. *Adv Virus Res* 44: 305-356, 1994.
57. Parker JN, Zhao W, Askins KJ, Broker TR and Chow LT: Mutational analyses of differentiation-dependent human papillomavirus type 18 enhancer elements in epithelial raft cultures of neonatal foreskin keratinocytes. *Cell Growth Differ* 8: 751-762, 1997.
58. Zhao W, Chow LT and Broker TR: A distal element in the HPV-11 upstream regulatory region contributes to promoter repression in basal keratinocytes in squamous epithelium. *Virology* 253: 219-229, 1999.
59. Beger M, Butz K, Denk C, Williams T, Hurst HC and Hoppe-Seyler F: Expression pattern of AP-2 transcription factors in cervical cancer cells and analysis of their influence on human papillomavirus oncogene transcription. *J Mol Med (Berl)* 79: 314-320, 2001.



This work is licensed under a Creative Commons Attribution-NonCommercial-NoDerivatives 4.0 International (CC BY-NC-ND 4.0) License.